Evolution of the Moat Associated with the Secondary Eyewall Formation in a Simulated Tropical Cyclone

NANNAN QIN,[a,b,c] LIGUANG WU,[a,b,d] AND QINGYUAN LIU[e,f]

[a] *Department of Atmospheric and Oceanic Sciences, Fudan University, Shanghai, China*
[b] *Institute of Atmospheric Sciences, Fudan University, Shanghai, China*
[c] *State Key Laboratory of Severe Weather, Chinese Academy of Meteorological Sciences, Beijing, China*
[d] *Innovation Center of Ocean and Atmosphere System, Zhuhai Fudan Innovation Research Institute, Zhuhai, China*
[e] *Nanjing Joint Institute for Atmospheric Sciences, Nanjing, China*
[f] *Key Laboratory of Transportation Meteorology, CMA, Nanjing, China*

(Manuscript received 11 December 2020, in final form 20 September 2021)

Introduction

- Observational studies show that about 80% of TCs with maximum wind over 62 m/s in the western North Pacific and about 70% of Atlantic major hurricanes (over cat. 3) have concentric eyewalls. (Hawkins and Helveston 2004; Kossin and Sitkowski 2009)

- SEF: convection rainband outside the inner eyewall -> secondary eyewall
- In a barotropic model, the outer convection vorticity can be stretched into a symmetric vorticity band at 3-4 times the radius of the inner eyewall when the inner eyewall vorticity is over 6 times stronger than the outer vorticity. (Kuo et al., 2004 and 2008)
- In a region with filamentation time > 30 min and weak negative radial gradient of vorticity, the convective rainbands could induce a LLJ to form a secondary eyewall through the interaction with the surface flux. (Terwey and Montgomery 2008)

Introduction

- A persistent rainband with diabatic heating occurs outside of the primary eyewall could broaden the tangential wind and form a secondary eyewall.

- The mid- to low-level inflow caused by the diabatic heating of rainband can propagate the rainband inward and transport high AAM inward. Tangential wind can be spun up.

Introduction

- SEF is sensitive to the solid-phase hydrometeors structures in the eyewall (terminal velocity). (Zhu and Zhu 2015)

- SEF: the fallout of hydrometeors from the cumulus primary eyewall -> evaporative cooling and subsidence -> formation of moat and outer convection. (Tyner et al. 2018; Willoughby et al. 1982; Zhu et al. 2015)

- The rapid filamentation dynamics played a secondary role in the organization of the moat by suppressing deep convection. (Wang 2008)

- To investigate the evolution of the SEF by focusing on the influences of inner-core structures and hydrometeor cooling processes on the associated moat evolution.

WRF Configuration

Typhoon Matsa (2005)

Semi-idealized simulation

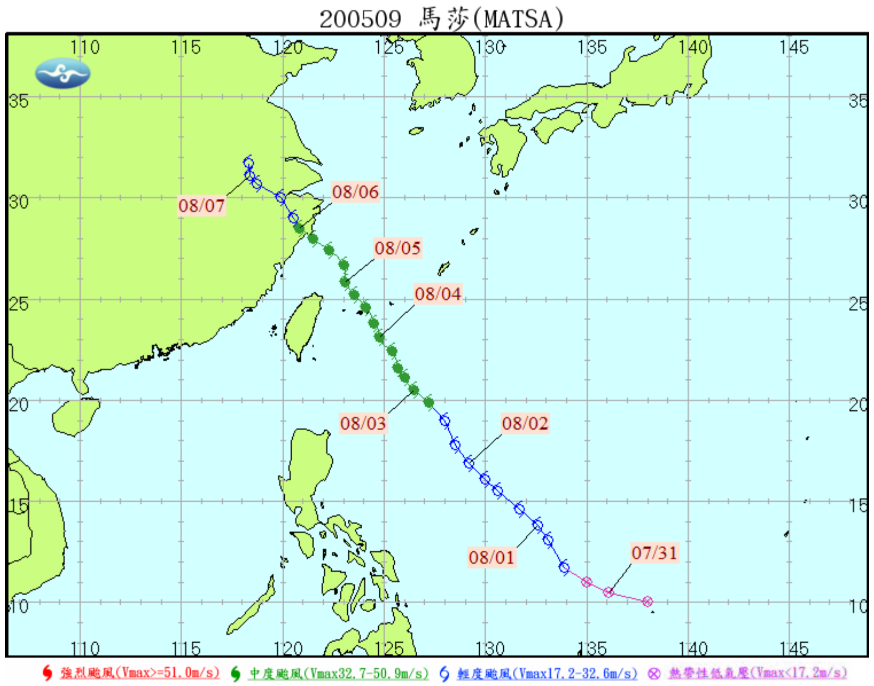

Version	3.2.1
Domains	5, d03 to d05 are moving
Grid size	27, 9, 3, 1, 1/3 (km)
Initial time	2005-08-05 00 Z
Integration period	72 hours
Eta levels	75
Model top	50 hPa
Cumulus scheme	Kain–Fritsch (d01 only)
Microphysics scheme	WSM6 (WSM3 for d01)
Longwave scheme	RRTM
Shortwave scheme	Dudhia
Land surface scheme	Noah
PBL Scheme	YSU
Boundary update cycle	6 hr (20-day low-pass filter)
DATASET	NCEP FNL (resolution: 1^{o})

WRF Configuration
Typhoon Matsa (2005)

Semi-idealized simulation

1. conducted a real-case simulation.
2. spin up for 12 hours.
3. A azimuthal-mean vortex with $\bar{V} = 29\ m/s$ at $r = 54\ km$ was put into the background.
4. large-scale condition: NCEP FNL with 20-day low-pass filter.
5. Integrated with open ocean at $SST = 29^{o}C$.

Version	3.2.1
Domains	5, d03 to d05 are moving
Grid size	27, 9, 3, 1, 1/3 (km)
Initial time	2005-08-05 00 Z
Boundary update cycle	6 hr (20-day low-pass filter)
DATASET	NCEP FNL (resolution: 1^{o})
SST	29^{o}C (fixed)

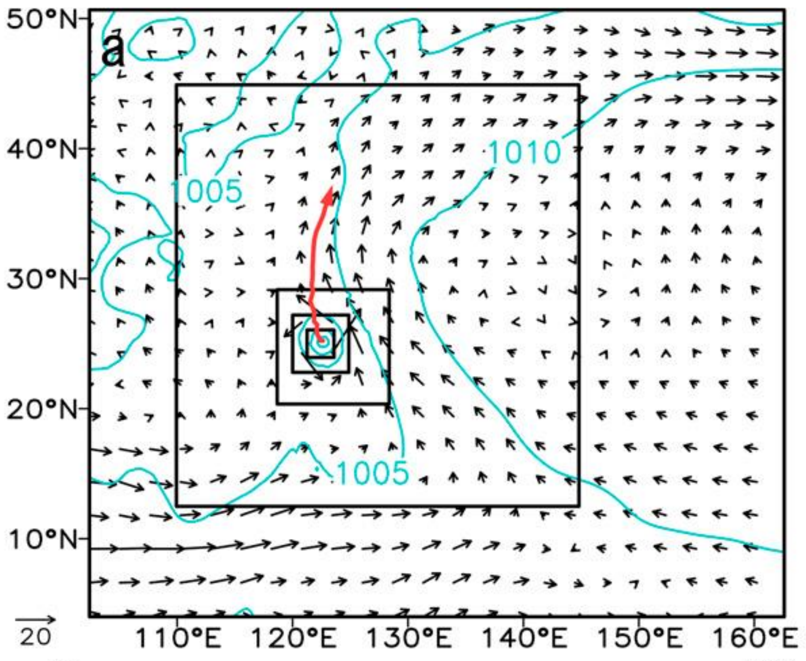

Overview of the simulated SEF

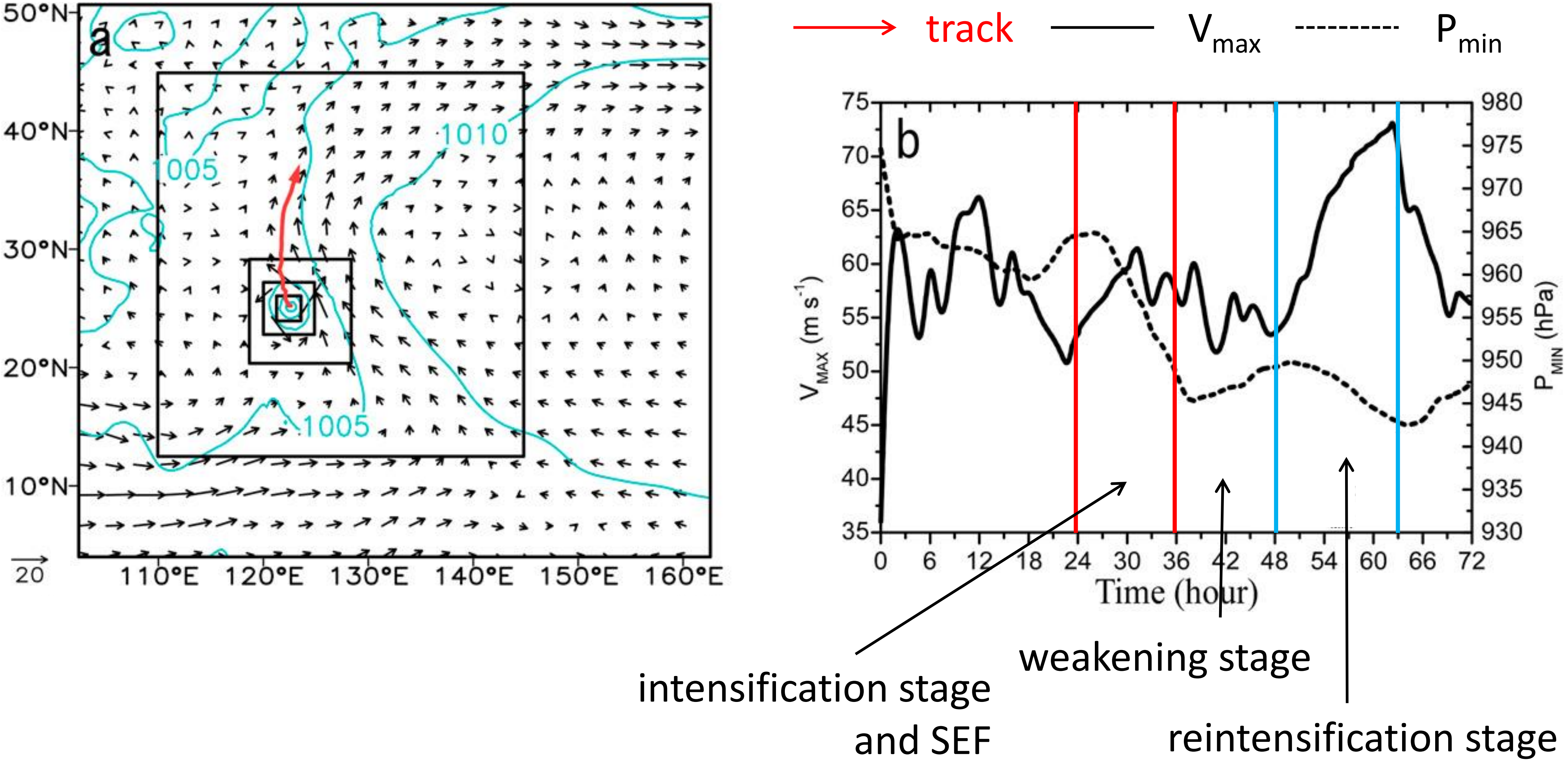

Overview of the simulated SEF

Azimuthal-mean

RMW

SEF

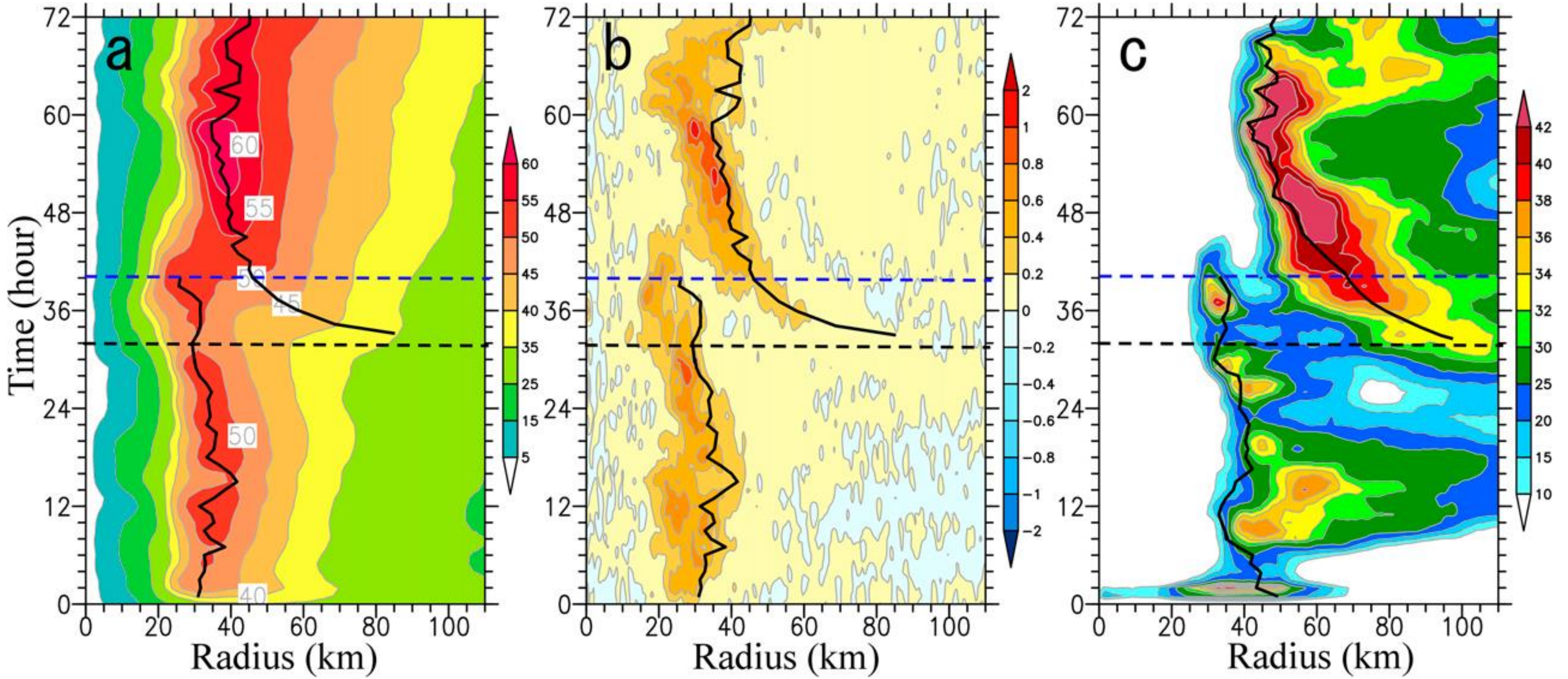

v at z = 0.5 km

w at z = 0.5 km

dB*Z* at at z = 5 km

Overview of the simulated SEF

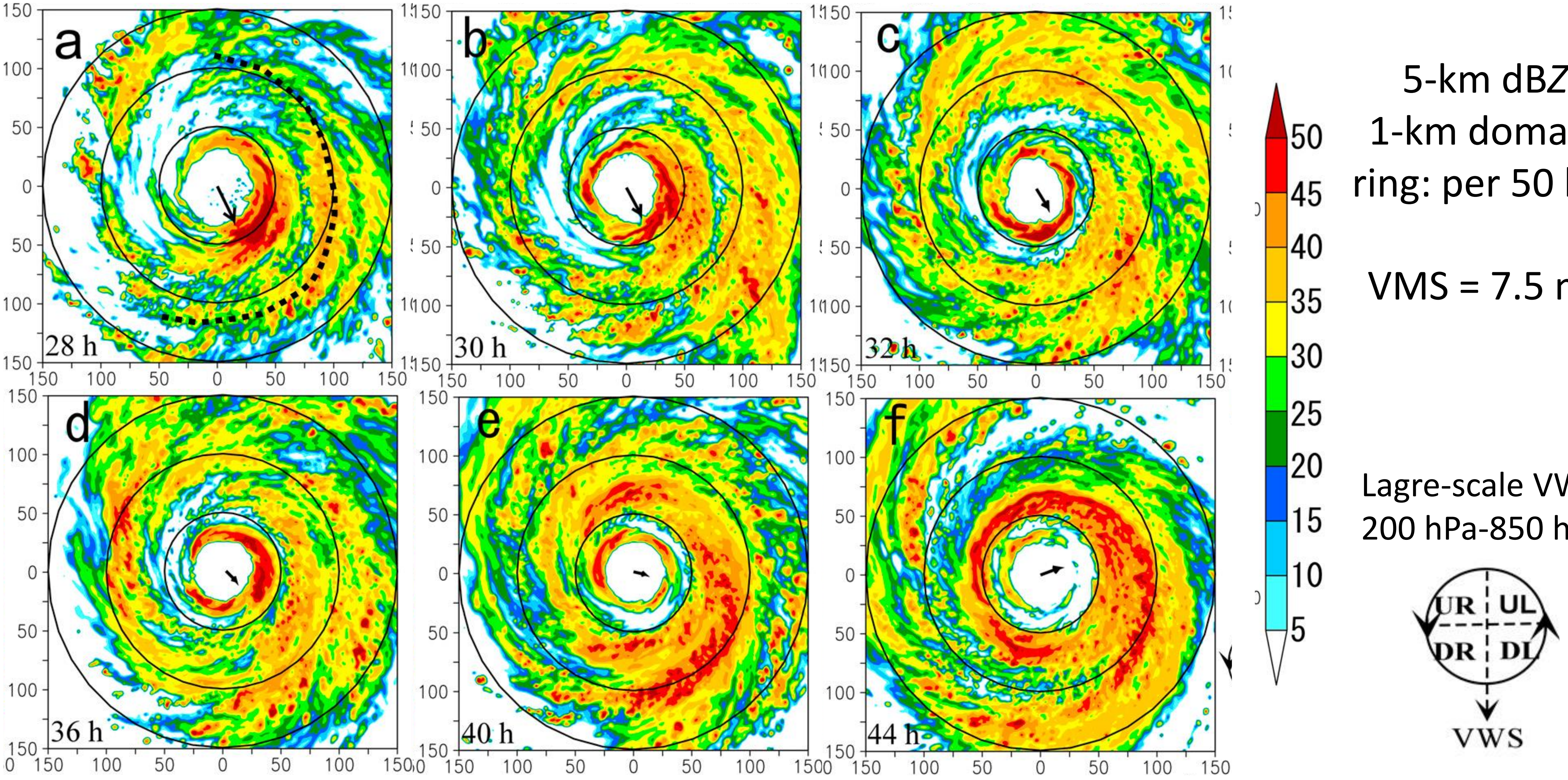

5-km dBZ
1-km domain
ring: per 50 km

VMS = 7.5 m/s

Lagre-scale VWS
200 hPa-850 hPa

Overview of the simulated SEF

Azimuthal-mean
color: w
vector: u, w
contour: q_{ice}
—— : RMW

W outside the inner eyewall was initially dominated by stratiform cloud and then by the convective cloud because the upward motion intensifies and contracts inward.
(Wang et al. 2019; Yu et al. 2020)

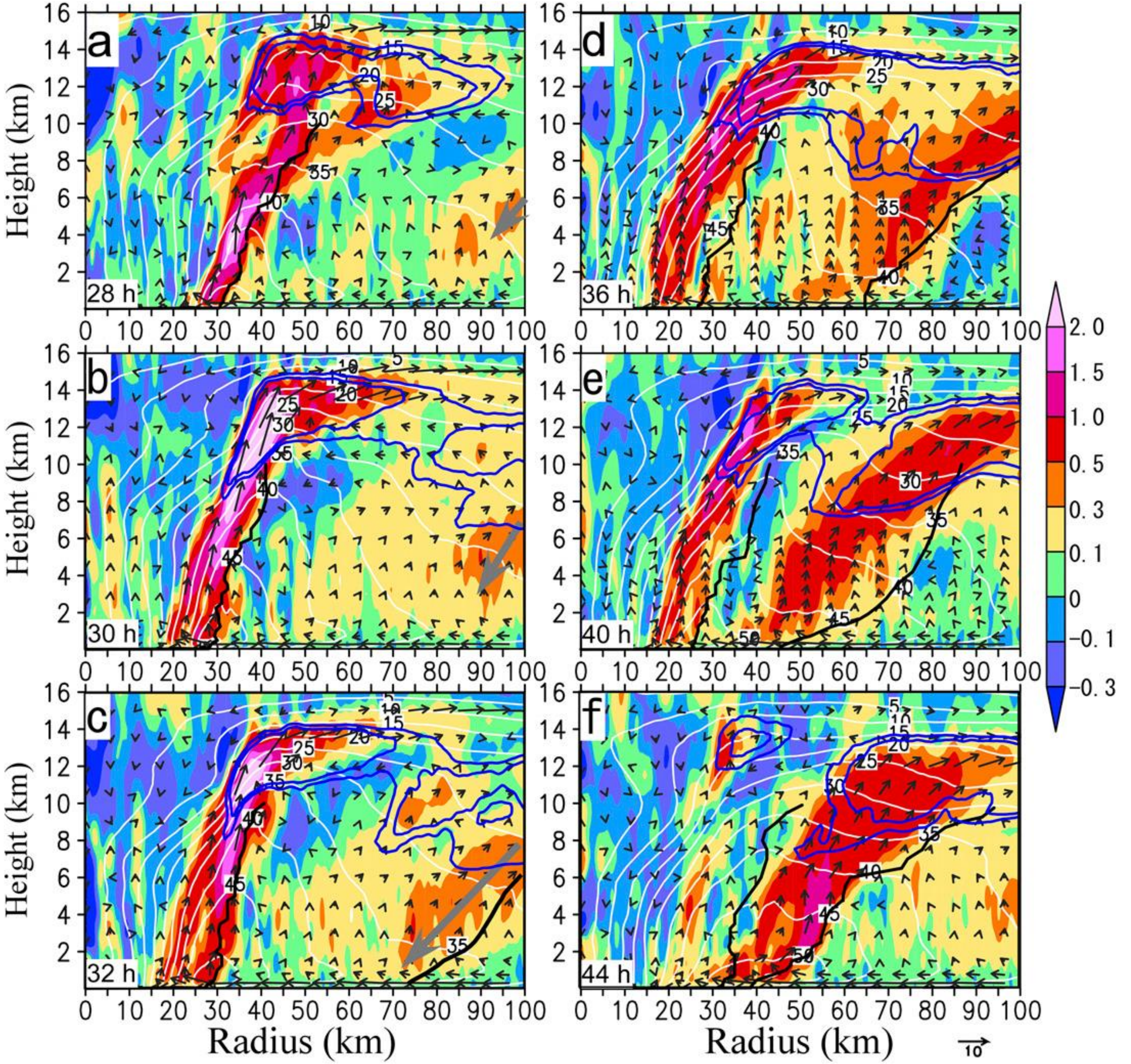

Evolution of the moat and the spiral rainband

Buoyancy:

$$B = g\left[\frac{\theta_v'}{\theta_{v0} + \theta_v^{0,1}} + (\kappa - 1)\frac{p'}{p_0 + p^{0,1}} - q'\right]$$

Thermal Dynamic Water loading

$A = A(r, \lambda, z)$
A_0 : average over d01 (501 x 501 km)
A^0 : wavenumber 0 component
A^1 : wavenumber 1 component
$A' = A - A_0 - A^0 - A^1$
$q = q_c + q_r + q_i + q_s + q_g$

Evolution of the moat and the spiral rainband

Upshear-right quadrant-mean

30 hr

—— : updraft

------- : downdraft

$\boldsymbol{\theta_v'}$

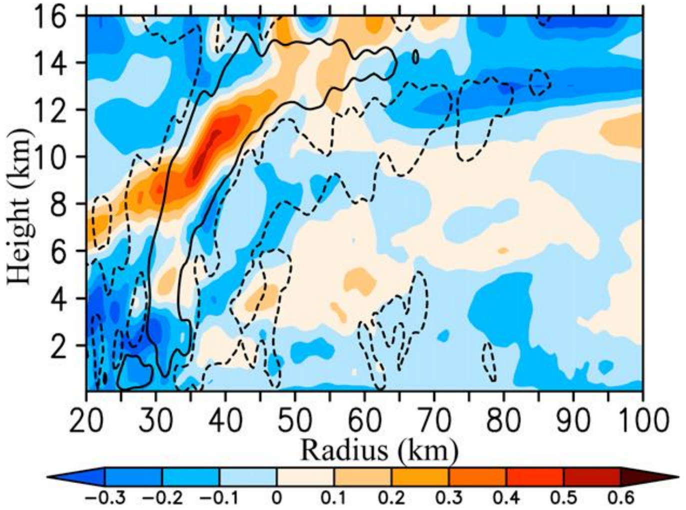

$$\frac{1}{\rho}\frac{\partial p'}{\partial z}$$

w tendency

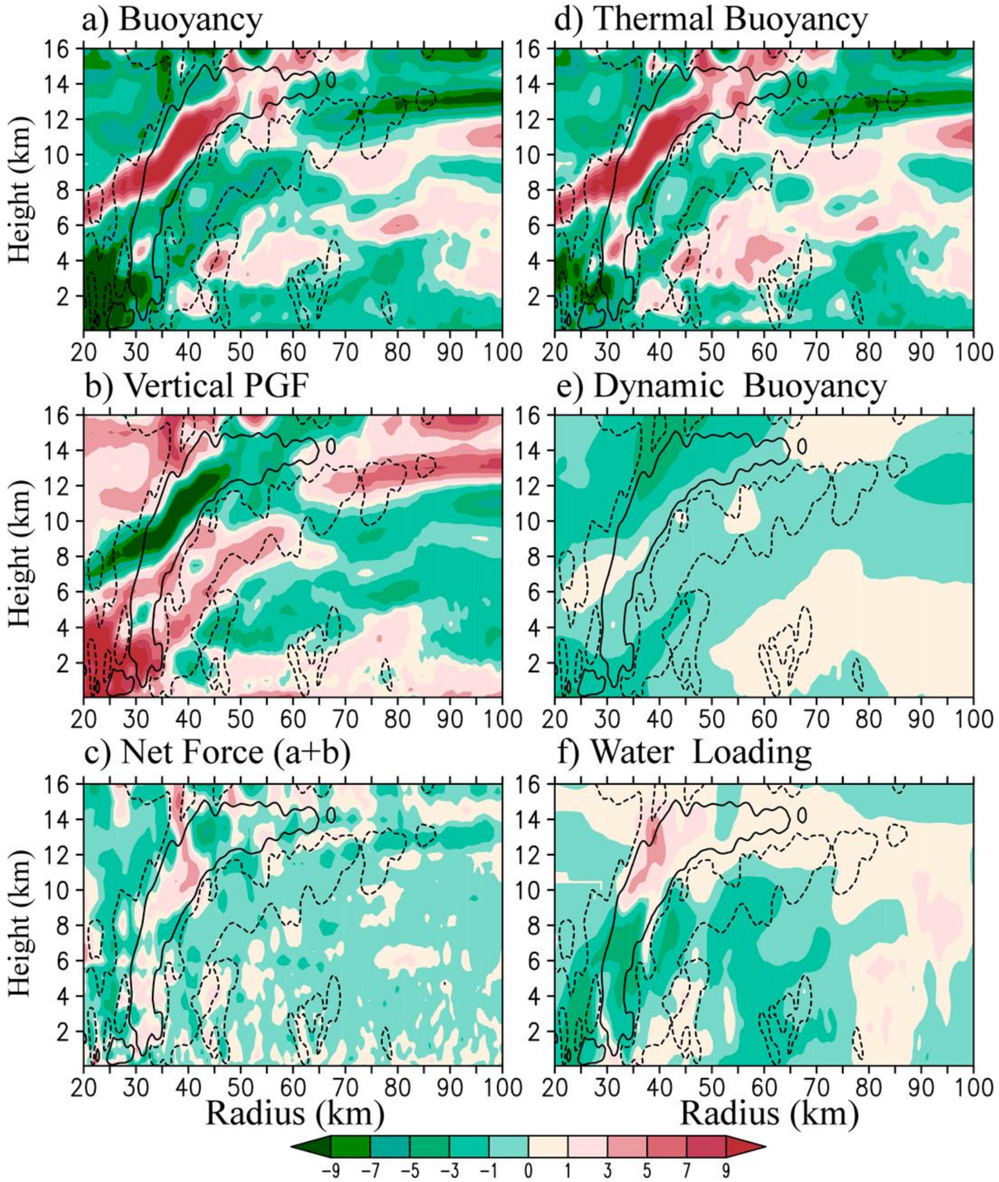

$$\frac{g\theta_v'}{\theta_{v0} + \theta_v^{0,1}}$$

$$\frac{(\kappa - 1)gp'}{p_0 + p^{0,1}}$$

$$gq'$$

Evolution of the moat and the spiral rainband

Upshear-right quadrant-mean

30 hr

—— : updraft

------- : downdraft

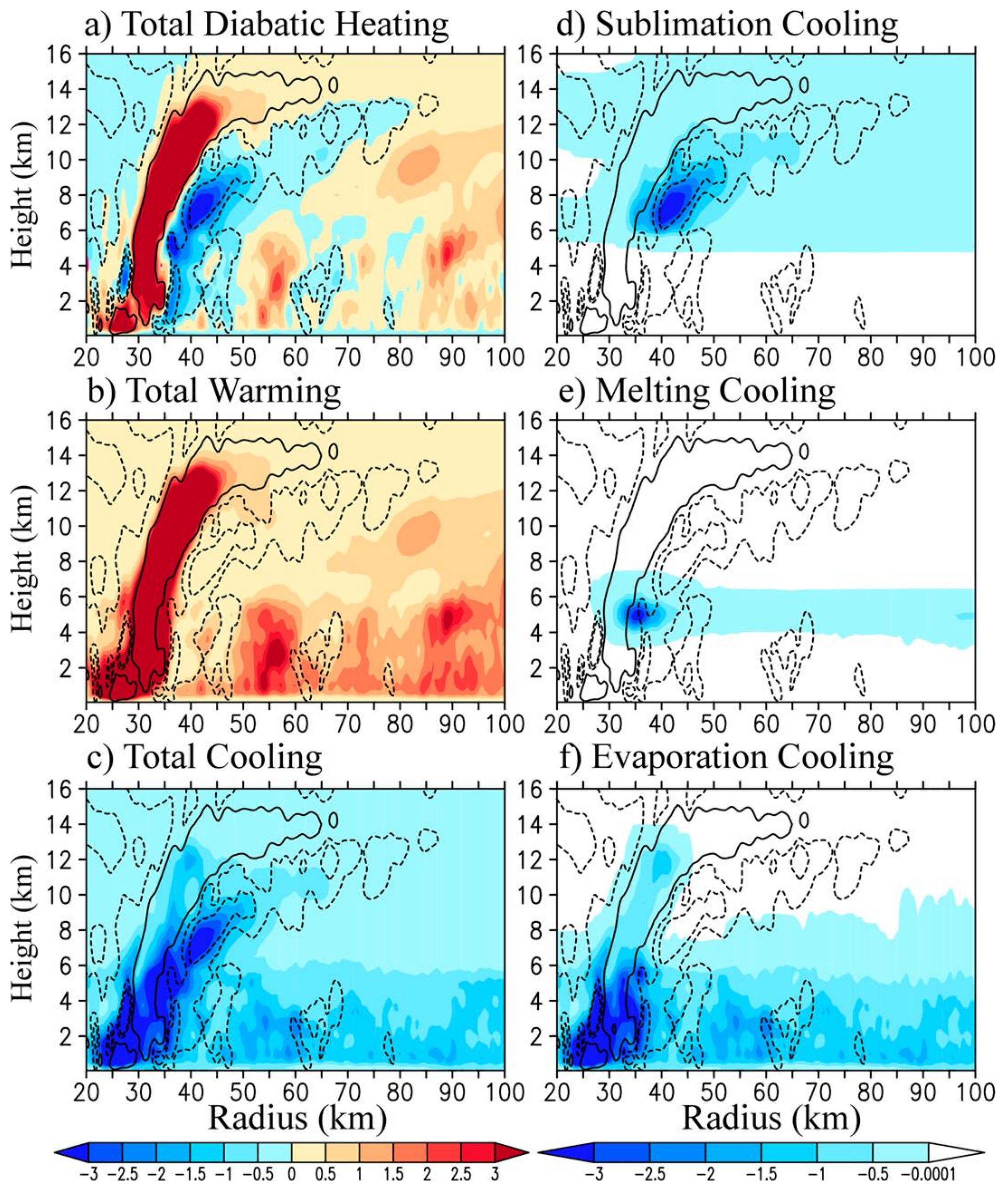

Evolution of the moat and the spiral rainband

Use **Sawyer-Eliassen Equation** to evaluate the secondary circulation in response to the specific cooling.

$$\frac{\partial}{\partial r}\left[\frac{\chi}{\rho r}\frac{\partial b}{\partial z}\frac{\partial \psi}{\partial r}-\frac{\chi}{\rho r}\frac{\partial b}{\partial r}\frac{\partial \psi}{\partial z}\right]+\frac{\partial}{\partial z}\left[\left(\chi\xi\zeta_a-\frac{C\chi}{g}\frac{\partial b}{\partial r}\right)\frac{1}{\rho r}\frac{\partial \psi}{\partial z}-\frac{\chi}{\rho r}\frac{\partial b}{\partial r}\frac{\partial \psi}{\partial r}\right]=g\frac{\partial \chi^2 Q}{\partial r}+\frac{\partial C\chi^2 Q}{\partial z}-\frac{\partial \chi\xi F_\lambda}{\partial r}$$

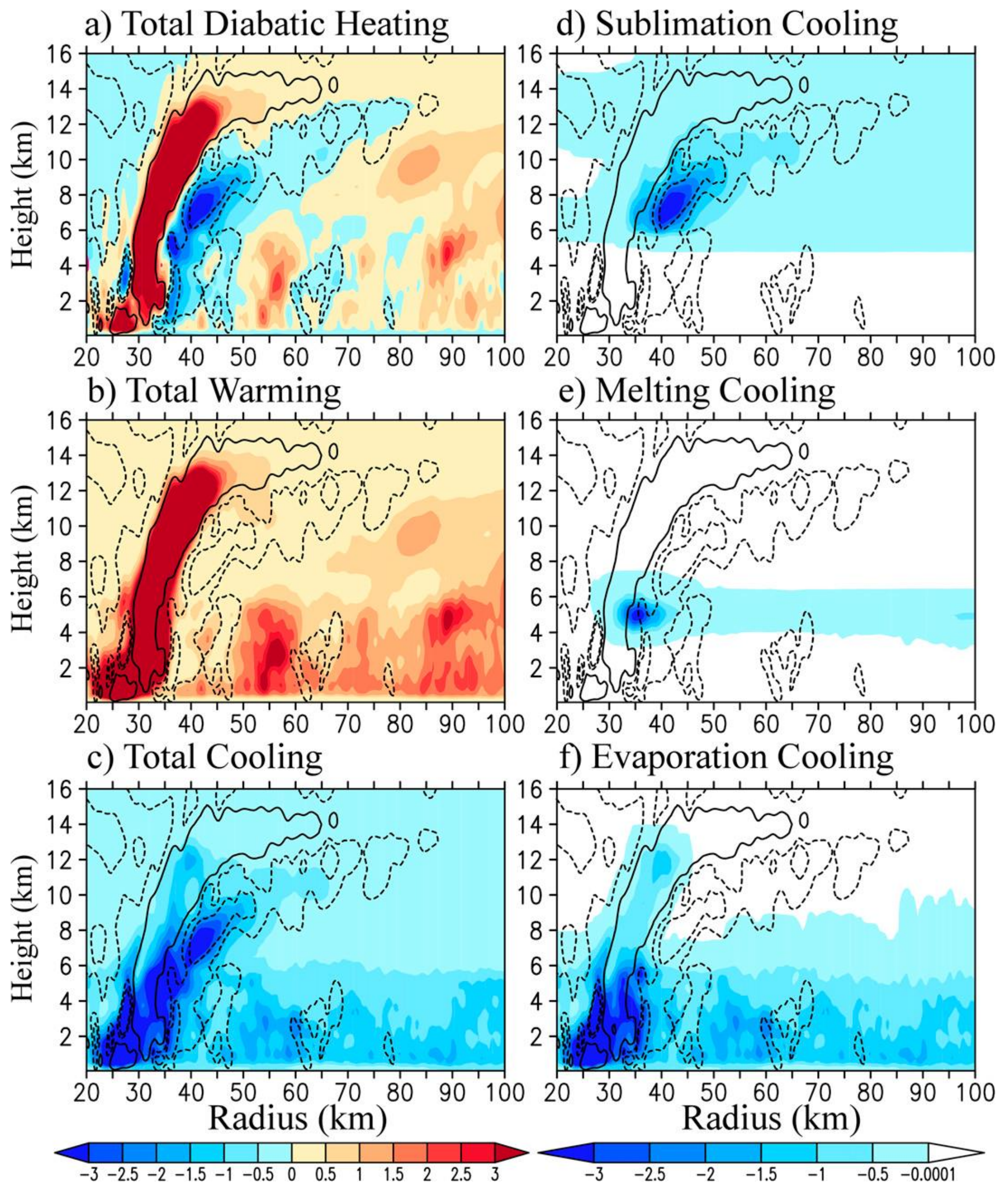

Evolution of the moat and the spiral rainband

Use **Sawyer-Eliassen Equation** to evaluate the secondary circulation in response to the specific cooling.

$$\frac{\partial}{\partial r}\left[\frac{\chi}{\rho r}\frac{\partial b}{\partial z}\frac{\partial \psi}{\partial r} - \frac{\chi}{\rho r}\frac{\partial b}{\partial r}\frac{\partial \psi}{\partial z}\right] + \frac{\partial}{\partial z}\left[\left(\chi\xi\zeta_a - \frac{C\chi}{g}\frac{\partial b}{\partial r}\right)\frac{1}{\rho r}\frac{\partial \psi}{\partial z} - \frac{\chi}{\rho r}\frac{\partial b}{\partial r}\frac{\partial \psi}{\partial r}\right] = g\frac{\partial \chi^2 Q}{\partial r} + \frac{\partial C\chi^2 Q}{\partial z} - \frac{\partial \chi\xi F_\lambda}{\partial r}$$

color: w

contour: u

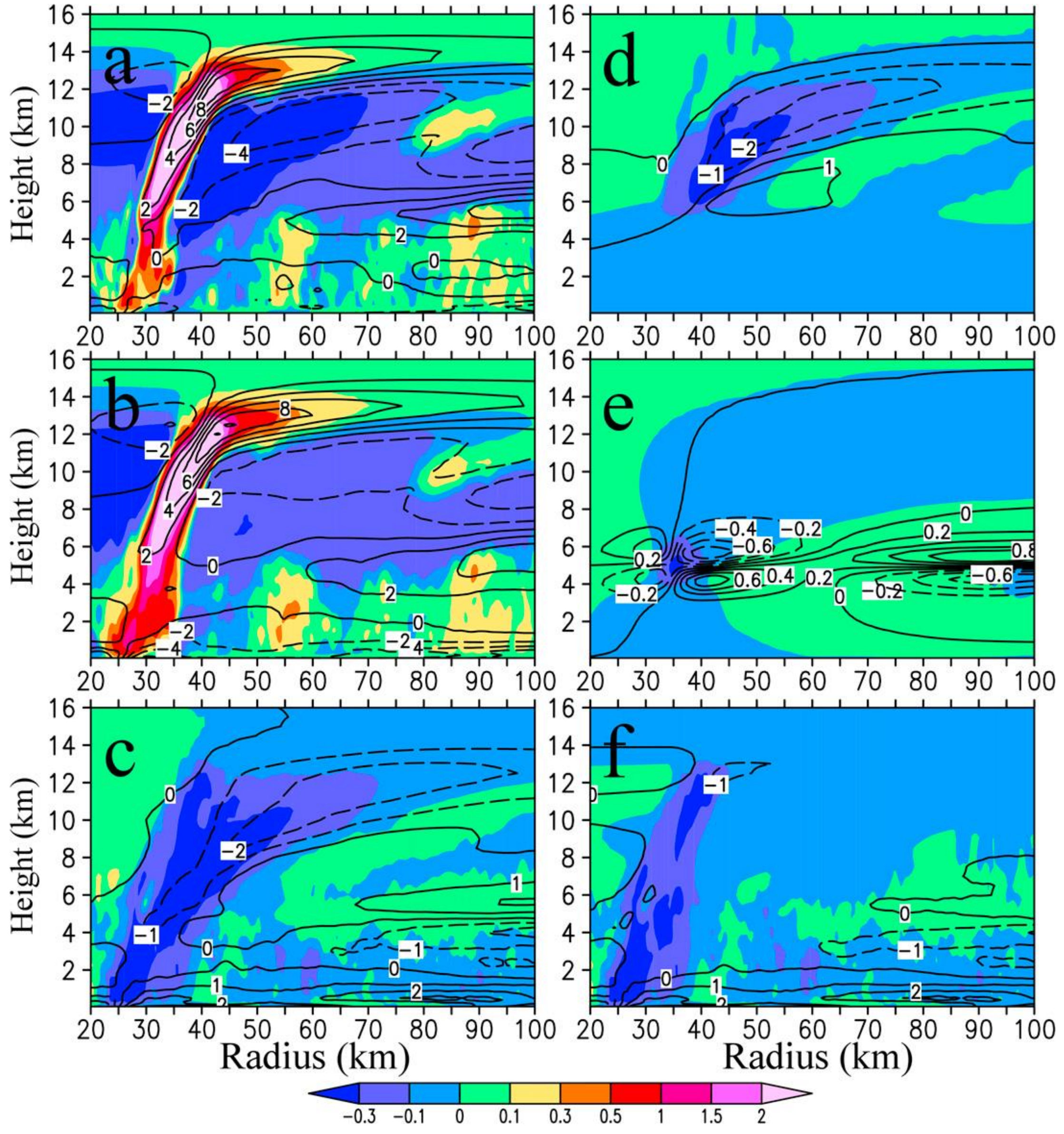

Evolution of the moat and the spiral rainband

color: Diabatic heating
contour: w

color: Bouyancy
contour: w

S-E equation
color: w
contour: u

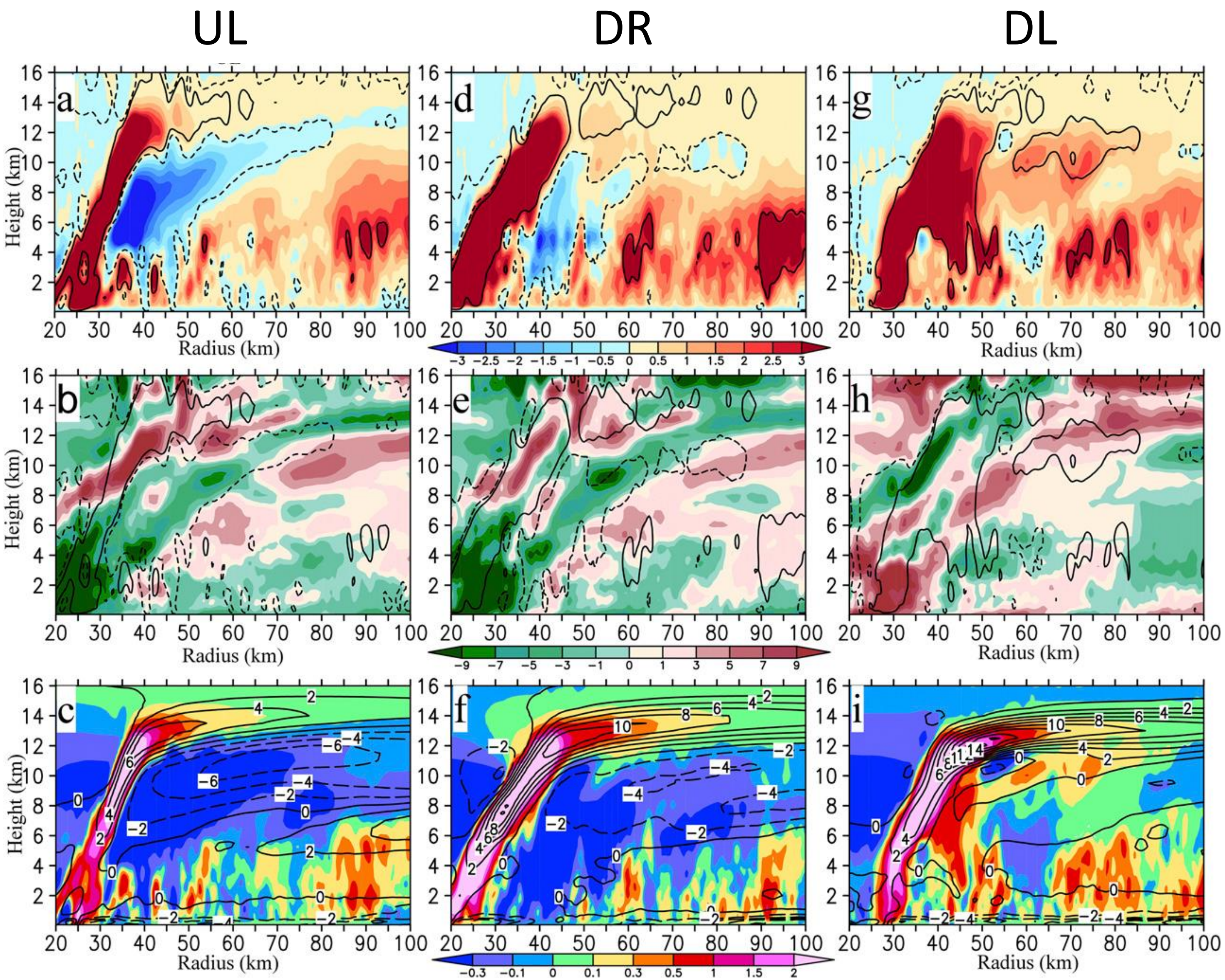

Evolution of the moat and the spiral rainband

Quadrant-mean
30 hr
color: RH
streamlines: u, w
contour: inflow

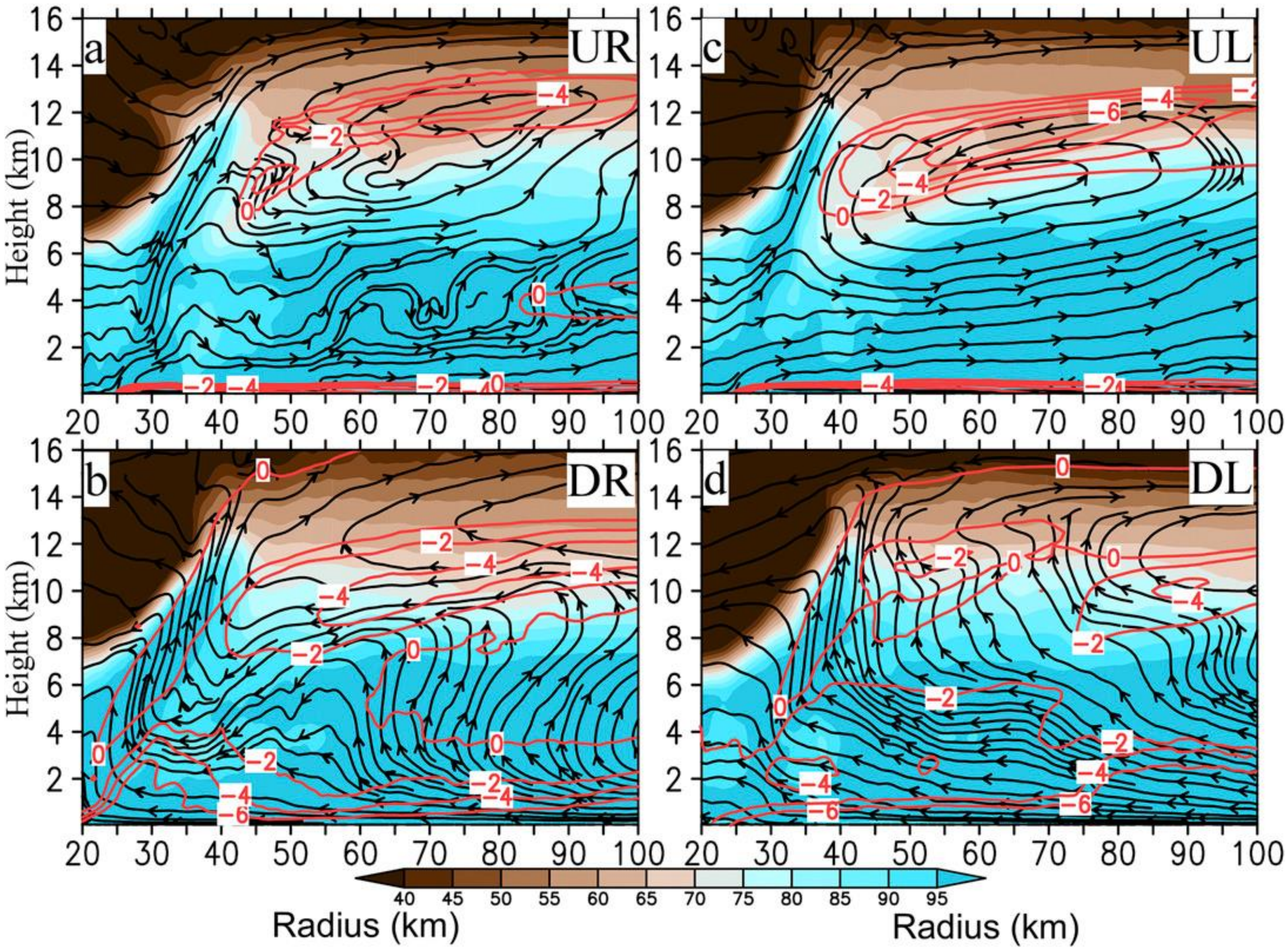

Evolution of the moat and the spiral rainband

Quadrant-mean
30 hr
color: w

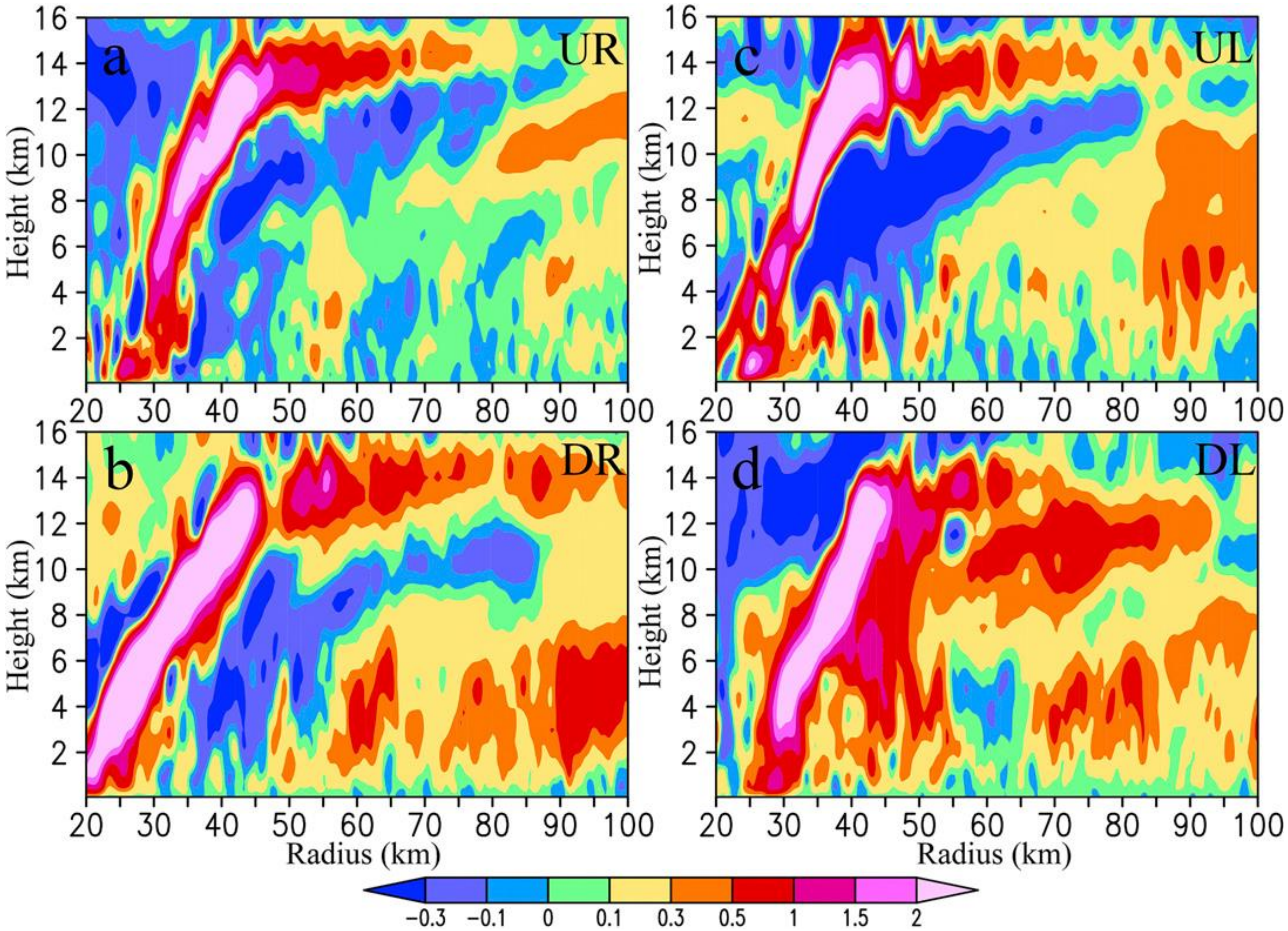

Evolution of the moat and the spiral rainband

r = 50~75 km mean

z = 10~12 km mean
color: w
contour: u

z = 10~12 km mean
color: Diabatic cooling
contour: w

z = 14~15 km mean
color: q_i (eyewall anvil)
contour: w

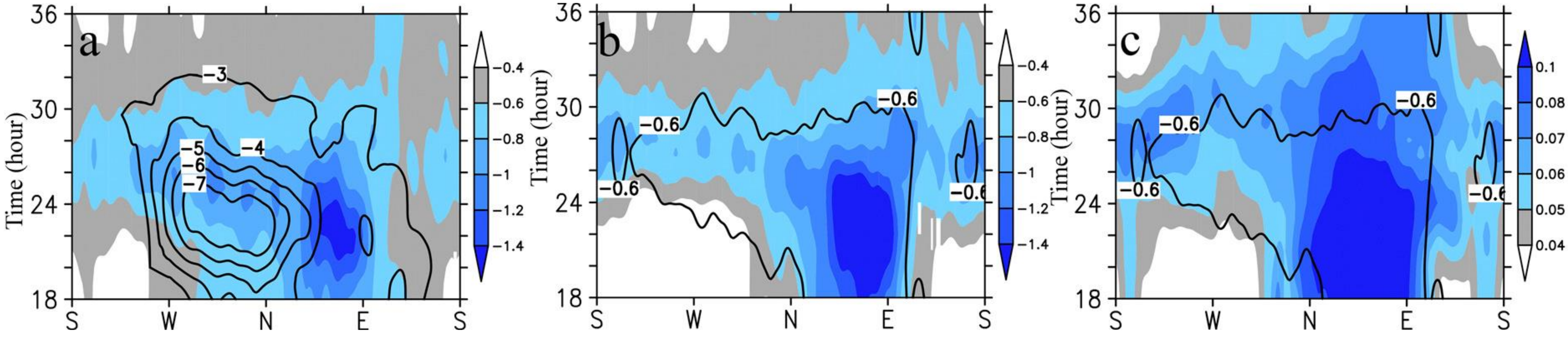

Evolution of the moat and the spiral rainband

Filamentation time by t = 26~32 h mean and azimuthal mean

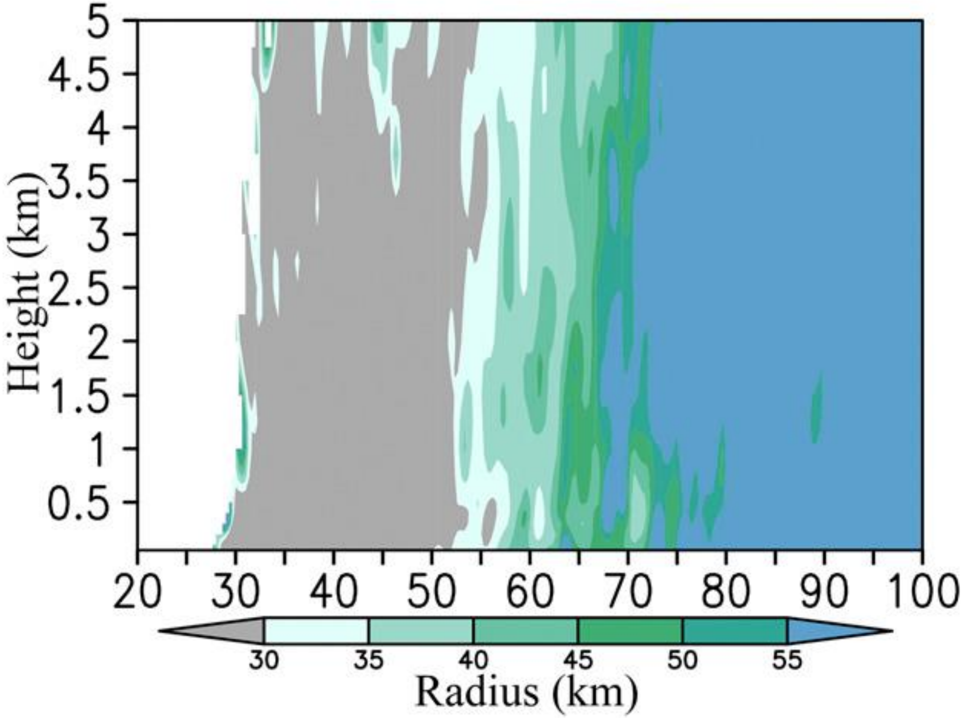

Filamentation time:

$$\tau_{fil} = 2(S_1^2 + S_1^2 - \zeta^2)^{-\frac{1}{2}}$$

$$for \quad S_1^2 + S_1^2 > \zeta^2$$

(strain-domanited)

S_1 、S_2 : deformation

ζ : vorticity

The rapid filamentation time (<30 min) outside the inner eyewall is important to the moat formation by distorting and suppressing the convection.

(Rozoff et al. 2006; Wang 2008, 2009)

Evolution of the moat and the spiral rainband

Axisymmetricity parameter between 2 ~ 6 km

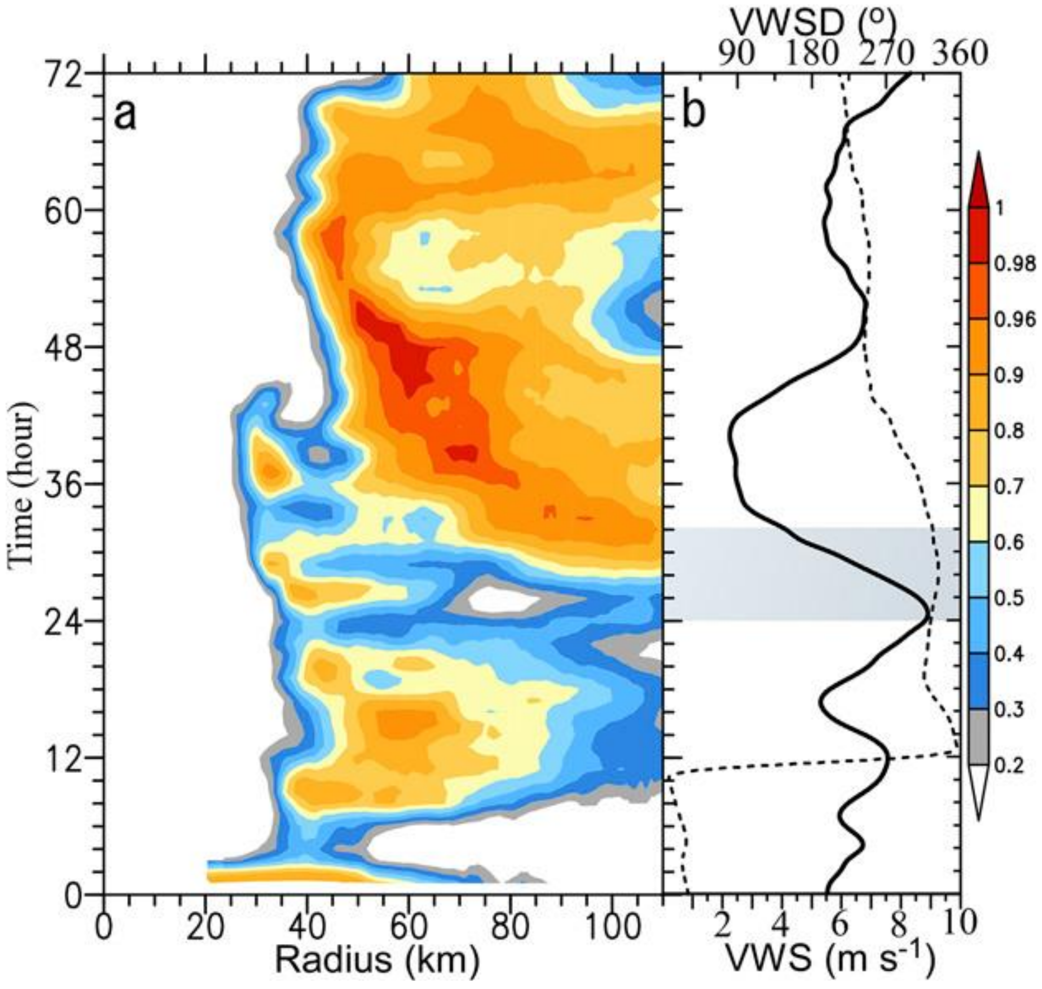

VWS speed

VWS direction

Axisymmetricity parameter

$$= \frac{\text{azimuthal mean } \mathrm{K_E}}{total\ K_E}$$

Conclusions

Formation of moat:

1. The inner eyewall updraft becomes strong with a upper-level anvil.
2. Upper-level outflow brings hydrometers outward.
3. Upper-level inflow brings the dry air inward and promotes sublimation cooling.
4. The diabatic cooling leads to negative buoyancy and subsidence.
5. Sublimation, melting, evaporation cooling enhance the negative buoyancy and subsidence.

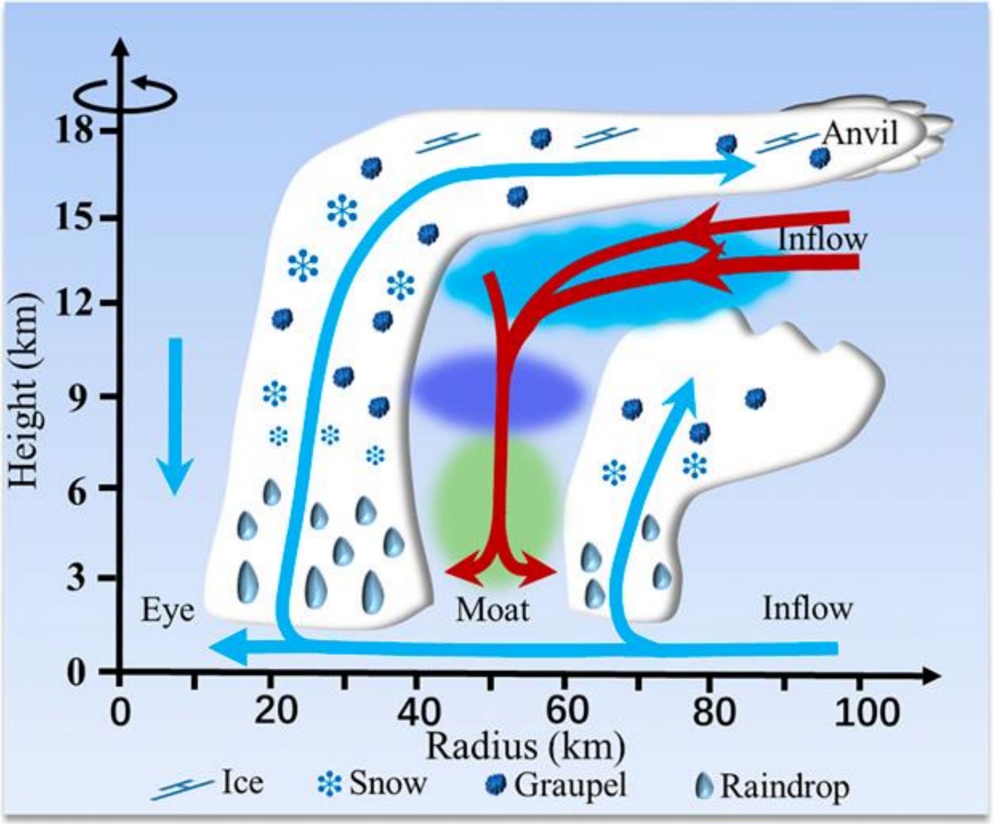

The reduction of the VWS and the rapid filamentation zone provide a favorable condition for the axisymmetrization of the outer convective rainband.